Soft Matter

PAPER

View Article Online
View Journal | View Issue

Cite this: *Soft Matter*, 2023, **19**, 2919

Membrane permeabilization can be crucially biased by a fusogenic lipid composition – leaky fusion caused by antimicrobial peptides in model membranes†

Katharina Beck, Janina Nandy and Maria Hoernke *

Induced membrane permeabilization or leakage is often taken as an indication for activity of membrane-active molecules, such as antimicrobial peptides (AMPs). The exact leakage mechanism is often unknown, but important, because certain mechanisms might actually contribute to microbial killing, while others are unselective, or potentially irrelevant in an *in vivo* situation. Using an antimicrobial example peptide (cR_3W_3), we illustrate one of the potentially misleading leakage mechanisms: leaky fusion, where leakage is coupled to membrane fusion. Like many others, we examine peptide-induced leakage in model vesicles consisting of binary mixtures of anionic and zwitterionic phospholipids. In fact, phosphatidylglycerol and phosphatidylethanolamine (PG/PE) are supposed to reflect bacterial membranes, but exhibit a high propensity for vesicle aggregation and fusion. We describe the implications of this vesicle fusion and aggregation for the reliability of model studies. The ambiguous role of the relatively fusogenic PE-lipids becomes clear as leakage decreases significantly when aggregation and fusion are prevented by sterical shielding. Furthermore, the mechanism of leakage changes if PE is exchanged for phosphatidylcholine (PC). We thus point out that the lipid composition of model membranes can be biased towards leaky fusion. This can lead to discrepancies between model studies and activity in true microbes, because leaky fusion is likely prevented by bacterial peptidoglycan layers. In conclusion, choosing the model membrane might implicate the type of effect (here leakage mechanism) that is observed. In the worst case, as with leaky fusion of PG/PE vesicles, this is not directly relevant for the intended antimicrobial application.

Received 24th December 2022,
Accepted 14th March 2023

DOI: 10.1039/d2sm01691e

rsc.li/soft-matter-journal

The negatively charged cytoplasmic membrane of pathogenic microbes is often discussed as the selective target of cationic, antimicrobial peptides (AMPs) or biomimetic polymers.[1–3] At the membrane, the membrane-active compounds can induce a variety of perturbations. In mechanistic model studies aiming at antimicrobial activity, membrane permeabilization is often tested. However, there are many different leakage mechanisms and also other types of membrane perturbations. Each of them may either indeed contribute to antimicrobial activity in microbes, or may only occur in model studies, or may occur in microbes but without antimicrobial effect. This can hamper meaningful interpretation of model studies.[3–5] Therefore, it is crucial to distinguish different effects, as addressed here, in order to understand the relation between model studies and microbial activity.

Most natural and designed antimicrobial peptides and their synthetic mimics are generally understood to act by their physical–chemical properties, such as hydrophobicity and charge. We have reported before that the composition of the lipid membrane might play a decisive role for the induced type of membrane perturbation.[6] Here, we use the cyclic antimicrobial peptide cR_3W_3 to investigate vesicle leakage, aggregation, and fusion in commonly used model vesicles containing phosphatidylglycerol (PG) and phosphatidylethanolamine (PE). It was shown that small peptides, including the structural relative cRRRWFW are able to pass the outer layers, peptidoglycan or outer membranes of microbes and then presumably act on the cytoplasmic membrane.[2,7,8] These bacterial cytoplasmic membranes are rich in negatively charged PG-lipids and zwitterionic PE-lipids[9,10] so that mixtures of these two lipids are commonly employed to study membrane behavior in antimicrobial activity.[3,11] Fig. 1 shows the structures of the unsaturated lipids used in this work. It is important to keep in mind

Chemistry and Pharmacy, Albert-Ludwigs-Universität, Freiburg i. Br., Germany. E-mail: Maria.Hoernke@BIOSS.uni-freiburg.de

† Electronic supplementary information (ESI) available: Additional data characterizing vesicle aggregation, peptide-vesicle binding, lipid mixing, stability of monolayers containing PEG-lipids, promotion of vesicle fusion. See DOI: https://doi.org/10.1039/d2sm01691e

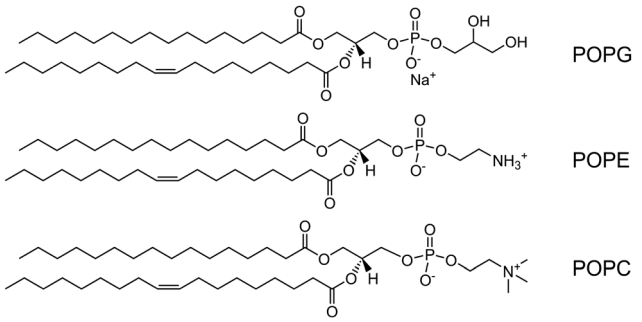

Fig. 1 Structure of the unsaturated lipids used in this work: 1-palmitoyl-2-oleoyl-*sn-glycero*-3-phospho-(1′-rac-glycerol) sodium salt (POPG), 1-palmitoyl-2-oleoyl-*sn-glycero*-3-phosphoethanolamine (POPE), and 1-palmitoyl-2-oleoyl-*sn-glycero*-3-phosphocholine (POPC).

that negatively charged vesicles have a tendency to aggregate upon addition of cationic compounds. Especially, we point out how PE-lipids can bias model studies of membrane leakage because of the pronounced fusogenicity of PE-rich membranes.

The high propensity of PG/PE membranes to aggregate and probably fuse upon addition of oppositely charged amphiphiles is not surprising. For vesicle–vesicle fusion, two barriers need to be overcome: first, both membranes need to make close contact.[12,13] This is facilitated by neutralization of the negative lipid head group charges upon binding of positively charged peptides.[14–17] Second, the formation of a fusion stalk locally requires high curvatures of the lipid layers. Different lipid species have higher or lower propensity for fusion stalks.[18] Especially PE-lipids with their relatively small head group and preference for local negative spontaneous curvature can therefore promote fusion.[18–20] This lipid-intrinsic tendency can be further enhanced by the binding and insertion of amphiphiles, such as AMPs.

Furthermore, POPG and POPE exhibit non-ideal mixing.[19] Therefore, compared to biological membranes with more diverse lipid composition, PG and PE-lipids could enhance certain membrane behavior, especially in binary model vesicles.

Many groups report vesicle aggregation and fusion (*e.g.*[21–25]) and some groups suspect,[26–29] establish,[5,30–32] or preclude[33,34] a link between leakage and fusion. In the current paper and for an antimicrobial polymer,[5] we describe that a part of the leakage observed in POPG/POPE model vesicles can be attributed to fusion or leaky fusion. Leaky fusion is unlikely in bacterial cytoplasmic membranes because membrane contacts needed for fusion are prevented by the bacterial peptidoglycan layers. Therefore, leaky fusion probably does not directly explain the activity of the peptide in microbes and needs to be identified or precluded.

In order to obtain more details on the the relation of leakage and fusion and the role of PE-lipids, we modify the lipid composition. Leakage and fusion are extensively characterized in POPG/POPE (1 : 1) membranes, but also in POPC-containing and cardiolipin-containing model membranes. In all the lipid compositions that we used, the fraction of negative lipid head group charges is identical. The electrostatic attraction should thus be the same, allowing us to investigate the role of the zwitterionic lipid. PG/PC mixtures provide an interesting comparison to PG/PE. PC-lipids are intrinsically much less prone to fusion,[18] because PC-lipids do not support negative spontaneous curvature as much as PE-lipids do.

To exemplify the role of membrane properties (*i.e.* different composition) for membrane perturbations such as leakage and fusion, we use an antimicrobial hexapeptide in the current study. cR_3W_3 is a cyclic hexapeptide containing three aromatic tryptophan residues and three cationic arginine amino acids.[7] The molecule fulfils the structural requirements of a cationic, amphipathic, antimicrobial peptide. cR_3W_3 is one of the most active members of a series of related cyclic hexapeptides and has been shown to have antimicrobial activity against Gram-positive and Gram-negative bacteria, while being only moderately haemolytic.[7] It can be assumed that the cyclic form studied here is more active than the linear form.[35]

Finger *et al.* studied the binding of cR_3W_3 and a series of related peptides to various mixed model membranes containing PG-lipids and PE-lipids. They focused on large, PG-rich lipid clusters induced by the peptides in mixed PG/PE membranes.[36,37] This is probably only one of many membrane perturbations. It was also shown that peripheral membrane proteins unbind from the membrane.[38] With the formation of nanotubes, Claro *et al.* propose another possible mechanism of action of a cyclic peptide.[39]

cR_3W_3 is an example of arginine-rich amphipathic peptides. Other arginine-rich peptides like oligoarginines and the TAT peptide are known as cell penetrating peptides that also induce membrane curvature.[40,41] For a closely related peptide, cRRRWFW, there are conflicting indications of induced leakage in model membranes[7] and no permeabilization or membrane translocation in bacteria.[2,42] Therefore, membrane permeabilization or leakage can be expected in model studies. Furthermore, related linear or cyclic hexapeptides have been found to localize to the membrane of *B. subtilis*, alter membrane fluidity locally, and cause peripheral membrane proteins to delocalize. It was suggested that membrane homeostasis and cell-wall synthesis are affected.[38,42]

In the current paper, we explore the role of the lipid composition for membrane leakage and a mechanism where leakage relies on membrane fusion, leaky fusion. For a better understanding of the role of PE-lipids in POPG/POPE (1 : 1) mixed vesicles for membrane permeabilization and fusion, three aspects have been investigated: (1) leakage behavior is thoroughly examined, aggregation and fusion are prevented to asses their role for the observed leakage. (2) The lipid composition is modified using phosphatidylcholine (PC) and cardiolipin (CL). (3) The implications of aggregation and fusion for data quality and options to judge data and ensure meaningful analysis are discussed.

This reveals the role of the model membrane composition for the relevance of model studies for antimicrobial activity and probably also for other membrane-related processes, such as drug delivery.

Materials and methods

Materials

1-Palmitoyl-2-oleoyl-*sn-glycero*-3-phosphocholine (POPC) and *N*-(carbonyl-methoxypolyethylene glycol-2000)-1,2-distearoyl-*sn-glycero*-3-phosphoethanolamine sodium salt (DSPE-PEG_{2000}) were purchased as lyophilized powder from Lipoid GmbH (Ludwigshafen, Germany). 1-Palmitoyl-2-oleoyl-*sn-glycero*-3-phosphoethanolamine (POPE), 1-palmitoyl-2-oleoyl-*sn-glycero*-3-phospho-(1′-rac-glycerol) sodium salt (POPG), and 1′,3′-bis[1-palmitoyl-2-oleoyl-*sn-glycero*-3-phospho]-glycerol sodium salt (TOCL), were purchased as chloroform solution from Avanti Polar Lipids (Alabaster, AL, USA). Lissamine Rhodamine B 1,2-dihexadecanoyl-*sn-glycero*-3-phosphoethanolamine triethylammonium salt (Rho-DHPE) and *N*-(7-nitrobenz-2-oxa-1,3-diazol-4-yl)-1,2-dihexadecanoyl-*sn-glycero*-3-phosphoethanolamine triethylammonium salt (NBD-PE) were purchased from Molecular Probes (Eugene, OR, USA). All lipids were used without further purification.

2-Amino-2-(hydroxymethyl)propane-1,3-diol (TRIS), sodium chloride (NaCl), and Triton X-100 obtained from Carl Roth GmbH (Karlsruhe, Germany) as well as Calcein and ethylenediaminetetraacetic acid (EDTA) obtained from Sigma-Aldrich (St. Louis, MO, USA) were used without further purification. The organic solvents chloroform and methanol (both HPCL grade) were purchased from Carl Roth GmbH (Karlsruhe, Germany).

Unless stated otherwise, solutions were prepared in standard TRIS buffer (10 mM TRIS, 110 mM NaCl, 0.5 mM EDTA, pH 7.4). The required electrolytes were weighed into a volumetric flask and dissolved in ultrapure water with a resistivity of 18.2 MΩ cm (Merck Millipore, Darmstadt, Germany). Before reaching the final volume, the pH value was carefully adjusted with HCl. After the final volume was reached, the pH value and the osmolarity were checked. To perform the leakage assay, an iso-osmotic calcein buffer (70 mM calcein, 10 mM TRIS, 0.5 mM EDTA, pH 7.4) was prepared. Under light protection, the electrolytes were weighed into a beaker, suspended in ultrapure water and carefully dissolved by slowly adding NaOH. The calcein solution was then transferred into a volumetric flask, the pH was finally adjusted with NaOH and ultrapure water was added to the final volume. The pH value and osmolarity were confirmed subsequently.

The synthetic cyclic hexapeptide c-RRRWWW (cR_3W_3) was custom-synthesized by GeneCust (Boynes, France) with a purity of ≥98% verified by HPLC. The peptide was dissolved in standard TRIS buffer at a concentration of 1 mM. This stock solution was stored at −20 °C and gently thawed and further diluted directly before the experiments to reach the final concentrations.

Liposome preparation

Liposomes used here as model membranes were prepared as described.[5] First, the required lipids were thoroughly dissolved in chloroform or chloroform/methanol (2 : 1) by gently shaking and required lipid mixtures were distributed over several glass vials. Afterwards, the organic solvent was removed by a rotary vacuum concentrator (RVC 2-18 CDplus, Martin Christ GmbH, Osterode am Harz, Germany) at 36 °C and additionally dried overnight under vacuum to produce thin lipid films. The composition was verified by weight and aliquots of the same solution were used to ensure identical lipid compositions in related experiments. Dry lipid films were either stored at −20 °C or directly processed further.

To prepare large unilamellar vesicles (LUVs) lipid films were rehydrated with standard TRIS buffer by vortexing for several minutes at room temperature. Whenever PEG-lipids were present, vortexing had to be avoided to prevent foaming. In these cases, the lipid suspensions were gently shaken at 400 rpm for two hours (Single TEC Control Shaker, INHECO, Martinsried, Germany). Then, five freeze–thaw cycles were performed. The liposomes were extruded through 80 nm polycarbonate membranes (Nuclepore Track-Etched Membranes, Whatman International Ltd, Maidstone, UK) at a temperature higher than the phase transition temperature of the lipid mixture. Whenever room temperature was appropriate, the LiposoFast hand extruder (Avestin, Ottawa, Canada) was used and 51 extrusion cycles were performed. Liposomes containing cardiolipin were extruded 15 times through two 80 nm polycarbonate membranes using a LIPEX Thermobarrel Extruder (Evonik Industries AG, Essen, Germany).

Calcein-filled liposomes are prepared by hydrating the lipid film with calcein buffer iso-osmotic to the standard TRIS buffer and following the regular procedure. To exchange the external calcein buffer for standard TRIS buffer, a PD-10 desalting column (GE Healthcare, Little Chalfont, UK) was used as described.[5] The ratio of entrapped and free calcein was determined and suitable fractions were pooled.

After preparation, a particle size of 105 ± 10 nm and a size distribution with a polydispersity index (PDI) < 0.1 were confirmed. For this, 5 μL of the freshly prepared vesicles suspension diluted with 1 mL TRIS buffer was characterized by dynamic light scattering as described in the following section. Finally, the lipid concentration of the liposome suspension was determined by Bartlett assay.[43]

Dynamic light scattering (DLS)

To determine the particle size (hydrodynamic diameter *Z*-average) and size distribution (PDI) of LUV suspensions, dynamic light scattering (DLS) was used.

Diluted liposome suspensions were examined with a Zetasizer Nano ZS (Malvern Panalytical Ltd., Worcestershire, United Kingdom) in a disposable cuvette (Semi-micro PMMA cuvette, Brand GmbH & Co. KG, Wertheim, Germany) at 25 °C. The instrument was equipped with a 633 nm helium–neon laser and the scattered light was detected at an angle of 173°. The liposomes size and size distribution were determined by the instrument software taking into account refractive index and viscosity of the buffer.

DLS was performed either directly after the preparation of the liposomes, or after incubation with the peptide as mentioned in the results section.

Fluorescence lifetime-based calcein leakage assay

Vesicle leakage was quantified using the soluble self-quenching fluorophore calcein and time-correlated single photon counting.[5,44]

Disposable polystyrene cuvettes (Sarstedt AG & Co., KG, Nümbrecht, Germany) filled with various concentrations up to 300 μM of the peptide freshly diluted in TRIS buffer were prepared. A reference sample containing only standard TRIS buffer was also prepared. The samples were placed on a rocking shaker (Single TEC Control Shaker, INHECO, Martinsried, Germany) at 400 rpm at 25 °C. Calcein-filled liposomes were added to start the incubation, so that a final lipid concentration of 30 μM was reached. After 10 minutes, 30 minutes, 1, 2, 5, and 24 hours, fluorescence decay curves were recorded with a FluoTime 100 (PicoQuant, Berlin, Germany). More precisely, a 467 nm laser diode pulsed at 1 MHz was used for excitation and fluorescence emission was recorded at 515 nm. Additionally, the particle size and size distribution were determined by DLS measurements after the experiment.

The acquired fluorescence decay curves can be deconvoluted from the instrument response function and fitted biexponentially using the TimeHarp 260 software (PicoQuant, Berlin, Germany):

$$F(f) = B_F \cdot e^{-t/\tau_F} + B_E \cdot e^{-t/\tau_E} \quad (1)$$

The amount of entrapped calcein in the liposomes is represented by the pre-exponential factor B_E with the associated fluorescence lifetime τ_E. B_F and τ_F represent the free calcein in the sample. Based on the amount of free calcein in the reference sample B_{F0}, the total leakage L_{total} can be calculated without the need for a fully leaked reference for a specific incubation time:[5,44]

$$L_{total} = \frac{(B_F - B_{F0})}{(B_F - B_{F0} + Q_{stat} \cdot B_E)}. \quad (2)$$

The denominator is a sum of the pre-exponential factors referred to as "sum of B" henceforth. Q_{stat} accounts for static quenching of calcein at high calcein concentration.

$$\text{Sum of } B = (B_F - B_{F0} + Q_{stat} \cdot B_E) \quad (3)$$

The pre-exponential factors are proportional to the effective calcein concentration and provide a measure for the fluorescence intensity that would reach the detector without the self-quenching and without any other disturbance. At a given concentration of dye, the sum of B should remain constant and is thus a useful parameter to asses whether the data is affected by changes in light scattering, turbidity, or sedimentation of larger particles, for instance.

In the current paper, data with a decrease in sum of B of more than 20% is omitted or marked.

NBD-rhodamine lipid mixing assay

Lipid mixing between liposomes can be monitored using a Förster resonance energy transfer (FRET) assay.[33,45,46] The fluoresence pair used here are NBD-labeled lipids (donor) and rhodamine-labeled lipids (acceptor).

To prepare double-labeled liposomes, 0.5 mol% of each FRET partner was added to the POPG/POPE film in the beginning of the liposome preparation. The remaining preparation was as described before. Directly before the experiment, labeled and unlabeled liposomes were mixed together to yield a final lipid concentration of 30 μM in a 1 : 4 (labeled : unlabeled) ratio with standard TRIS buffer. The experiment was performed on a LS 55 Fluorescence Spectrometer (PerkinElmer Inc., Norwalk, CT, USA) in quartz cuvettes (Hellma, Müllheim, Germany) at 25 °C and slow stirring. After excitation at a wavelength of 463 nm with a slit width of 10 nm, the emission spectrum was measured from 480–650 nm every 5 minutes. To start the measurement, the required amount of the peptide stock solution was added directly to the liposome-containing cuvette to reach the final peptide concentrations between 0.5 and 50 μM. In the end, 18 μL Triton X-100 were added and one last emission spectrum was recorded.

The intensity ratio R is the quotient of the maximum fluorescence intensities of NBD at 520 nm and of Rhodamine at 580 nm:

$$R = \frac{I_{NBD}}{I_{Rho}} = \frac{I(520\,\text{nm})}{I(580\,\text{nm})}. \quad (4)$$

The lipid mixing efficiency at a particular peptide concentration and incubation time was then calculated as

$$\text{Lipid mixing efficiency} = \frac{R - R_0}{R_\infty - R_0}, \quad (5)$$

taking into account the ratio before the addition of the peptide R_0 and after the addition of Triton R_∞.[33] Triton solubilizes the labeled and unlabeled liposomes into micelles and thereby increases the distance between the labeled lipids. With the ratio of labeled to unlabeled liposomes used here (1 : 4), a maximal value of approximately 0.4 can be expected.[5]

Isothermal titration calorimetry (ITC)

Isothermal titration calorimetry (ITC) was performed to characterise the interaction of the peptide with model membranes.

To this end, stock solutions of the respective peptide and liposomes were diluted separately with standard TRIS buffer to yield the required concentration. Then, the samples were pre-tempered and degassed for 4 minutes in the ThermoVac accessory device (Malvern Panalytical Ltd., Worcestershire, United Kingdom). 0.1 mM peptide solution was filled into the reaction cell of a VP-ITC MicroCalorimeter (Malvern Panalytical Ltd., Worcestershire, United Kingdom) and tempered to 25 °C. 5 mM liposome suspension was loaded into the syringe and injected in aliquots of 10 μL, with a duration of 20 s, in time steps of 600 s, stirred at 286 rpm.

The obtained raw thermograms were integrated and further analysed using MicroCal Data Analysis in Origin, version 7.0 (MicroCal, Northhampton, MA, USA). Heat of dilution was not taken into account. To estimate the apparent thermodynamic parameters of the interaction of lipids and peptides, the

built-in one-set-of-sites curve fitting model of the provided software was fitted to the sigmoidal isotherms.

Results

The impact of the antimicrobial peptide cR_3W_3 on different model membranes was investigated, focusing initially on leakage behavior in POPG/POPE (1 : 1) vesicles.

The content leakage from vesicles was quantified by time-correlated single photon counting using self-quenching calcein as a marker.[44] The advantage of this method is that the sum of B (see Methods section and ESI†) can be used to judge data quality. Furthermore, three types of information can be examined at once: (1) activity or dose-response, *i.e.* vesicle leakage represented as a function of concentration of added peptide (first column in Fig. 2), (2) lifetime of still entrapped calcein τ_E helps to distinguish all-or-none from graded leakage (second column in Fig. 2), (3) membrane permeabilization behavior over time may indicate the (re-)occurrence of leakage events (third column in Fig. 2).

Fast all-or-none leakage of POPG/POPE vesicles

Leakage induced by cR_3W_3 in POPG/POPE model vesicles was examined at increasing peptide concentration (1 μM to 300 μM) and for incubation times up to 24 hours (Fig. 2A–C).

Fig. 2A exhibits the characteristic, sigmoidal shape of the dose-response leakage curve as a function of peptide concentration. Vesicle leakage occurs with increasing concentration of the peptide with a steep onset between 3 and 10 μM cR_3W_3 followed by an apparent plateau. At 30 μM peptide concentration, leakage increases from approximately 50% after 10 minutes of incubation to more than 80% after 2 hours. At these very high L_{total} above 80%, the fit of the decay curves becomes invariant and these data points should not be interpreted quantitatively, *i.e.* are considered complete leakage.

We have to note that the samples with more than 10 μM cR_3W_3 are affected by aggregation up to the formation of visible particles (see Fig. S2, ESI†). Data points with decreased sum of B (eqn (3)) by more than 20% with respect to the initial value (Fig. S1, ESI†) are shown in grey and should not be evaluated quantitatively. Further information on leakage behavior becomes available by depicting the total leakage as a function of the lifetime of the still entrapped calcein on a reciprocal scale.[44] The lifetime of calcein entrapped in POPG/POPE vesicles, τ_E, remains constant at approximately 0.4 ns even with increasing leakage (Fig. 2B). This indicates that only two types of vesicles are present in the sample: intact vesicles with highly concentrated calcein and fully equilibrated ones. This is known as all-or-none (AON) leakage behavior.[44,47,48] For graded leakage,[47] the data points would be expected to coincide with the dashed diagonal line in the second column in Fig. 2.[44]

Evaluating the time course of leakage over several minutes and hours (third column in Fig. 2) distinguishes transient leakage from continuous leakage. For transient leakage, either asymmetric-packing stress or leaky fusion are discussed.[4] In continuous leakage, the leakage events or pores form continuously.[49] As shown in Fig. 2A and C, cR_3W_3 induces substantial leakage in POPG/POPE vesicles already after 10 minutes with only a slight further increase over time. This indicates transient leakage and we will argue that the most likely mechanism of leakage in POPG/POPE vesicles is leaky fusion.

Increase in particle size

DLS measurements reveal the particle size and size distribution in the liposome suspension upon addition of the peptide. Fig. 3 shows the Z-average size and polydispersity after incubating 30 μM vesicles with cR_3W_3 for 24 h.

In the sample containing POPG/POPE vesicles (Fig. 3A, red bars), the particle size increased slightly at 3 μM peptide concentration. At 10 μM, particle sizes increased substantially to several hundred nm and further at higher peptide concentrations. At peptide concentrations above 100 μM the aggregates were even visible to the eye (Picture S2, ESI†). The size distribution was very heterogeneous (symbols and right axis in Fig. 3). We attribute these changes to vesicle aggregation and fusion or similar changes in the liposome suspension that result in large scale membrane structures.

Lipid mixing indicates fusion of POPG/POPE vesicles

To distinguish aggregation of vesicles from membrane fusion, lipid mixing can be assessed by Förster resonance energy transfer (FRET) between NBD-labeled and rhodamine-labeled lipids. When liposomes containing both donor- and acceptor-lipids fuse with unlabeled vesicles, the fluorophores in the membrane are diluted, thereby reducing FRET. Strictly, lipid mixing does not prove full vesicle fusion.

Fig. 4 shows the total lipid mixing measured in POPG/POPE vesicles after the addition of the peptide. Lipid mixing occurred very rapidly within the first minutes of incubation and increased with peptide concentration. Above 3 μM cR_3W_3, substantial lipid mixing occurred. At higher concentrations, a plateau was reached at approximately 0.4. This value is the expected maximum for the ratio of labeled to unlabeled vesicles used here (1 : 4).[5] Vesicle leakage occurred at similar peptide concentrations.

The experiment is affected by multiple side effects and only reliable data is shown. Vesicle aggregation and light scattering decrease the detected fluorescence intensity, especially at higher peptide concentrations and incubation times longer than 11 minutes (Fig. S5, ESI†). In addition, the tryptophan side chains of cR_3W_3 seem to interfere with the FRET on which the assay is based (Fig. S5, ESI†). Although only short incubation times yield quantifiable data, it was possible to detect peptide-induced fusion or fusion intermediates involving mixing of lipids in POPG/POPE vesicles.

Because of concomitant leakage and expected problems with fluorescence intensity, proving or quantifying content mixing was not attempted.

Leakage decreases when vesicle aggregation and fusion are prevented

To determine if the aggregation and fusion are contributing to vesicle leakage, membrane–membrane contacts can be prevented by the incorporation of 4 mol% DSPE-PEG_{2000}.[5,33,50]

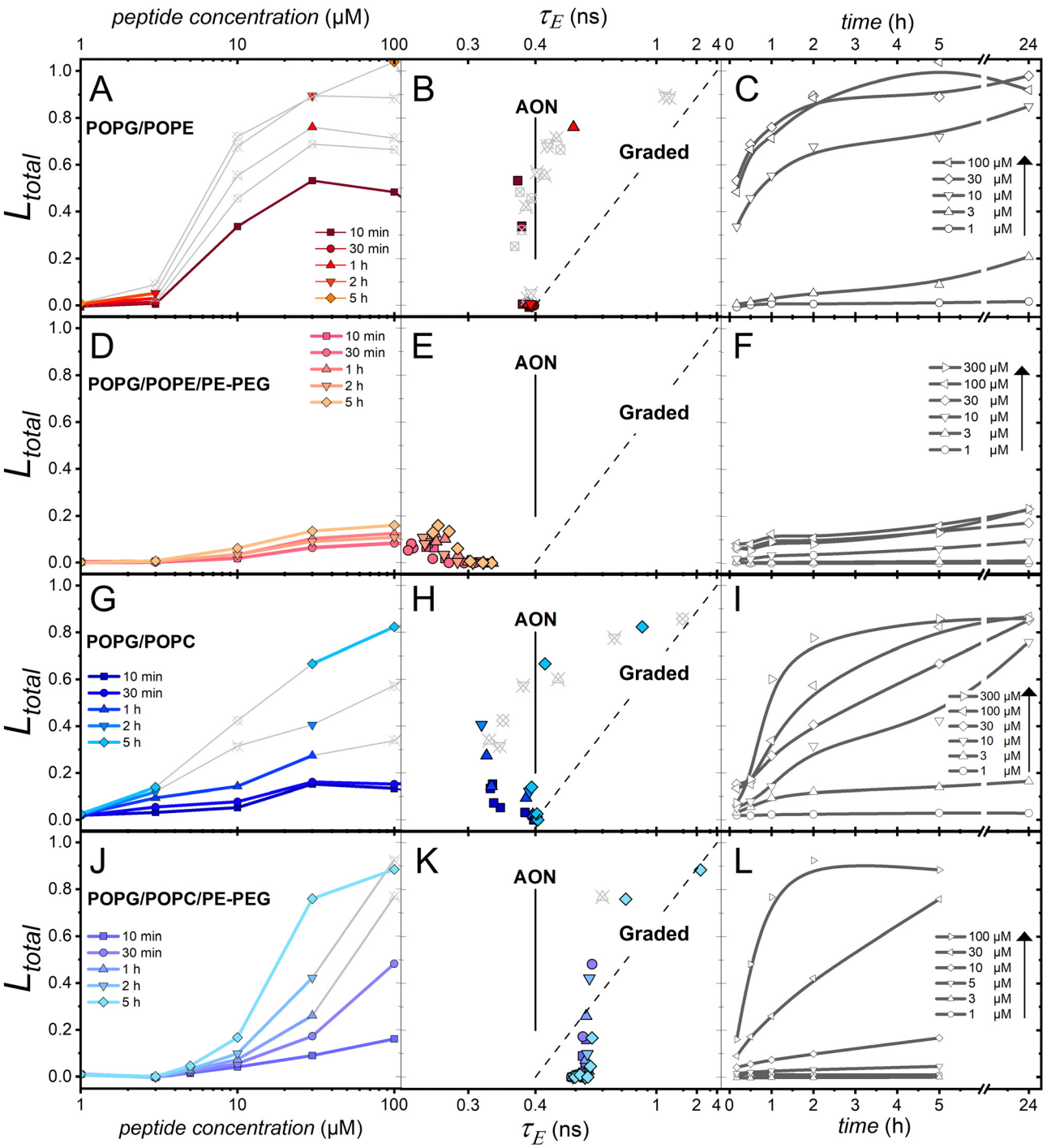

Fig. 2 Calcein leakage induced by different concentrations of cR_3W_3 in 30 μM POPG/POPE (50 : 50) (A–C), POPG/POPE/DSPE-PEG_{2000} (50 : 50 : 4) (D–F), POPG/POPC (50 : 50) (G–I), or POPG/POPC/DSPE-PEG_{2000} (50 : 50 : 4) (J–L). The left column shows total leakage as a function of peptide concentration at various incubation times. The middle column shows leakage as a function of the fluorescence lifetime of entrapped calcein dye, τ_E, on a reciprocal scale. The theoretical behaviour of AON (All-Or-None) and graded leakage and is shown as black lines. The right column shows total calcein leakage as a function of incubation time at different peptide concentrations. Data with a decrease in sum of *B* of more than 20% is omitted or depicted in grey (see Fig. S1, ESI†). The experiments were performed in standard TRIS buffer at 25 °C. The depicted data is a typical example of two or three experiments conducted at similar conditions, except for POPG/POPC/DSPE-PEG that did not yield stable vesicles in most preparations. Fig. S3 (ESI†) gives an impression of the fluctuations between data sets. The amounts of entrapped or free calcein in samples without addition of peptides do not decrease or increase, respectively, over time and fluctuate less than 3% within 5 hours and less than 6% within 24 hours.

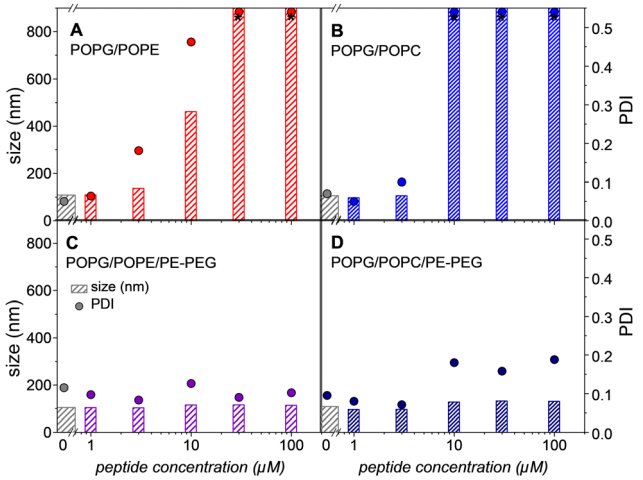

Fig. 3 *Z*-average size (bars) and polydispersity index (PDI) (dots) obtained by dynamic light scattering for (A): POPG/POPE (50 : 50) (red), (B): POPG/POPC (50 : 50) (blue), (C): POPG/POPE/DSPE-PEG_{2000} (50 : 50 : 4) (purple), and (D): POPG/POPC/DSPE-PEG_{2000} (50 : 50 : 4) (dark blue) vesicles after 24 h of incubation with various concentrations of cR_3W_3. The experiments were performed in standard TRIS buffer at 25 °C.

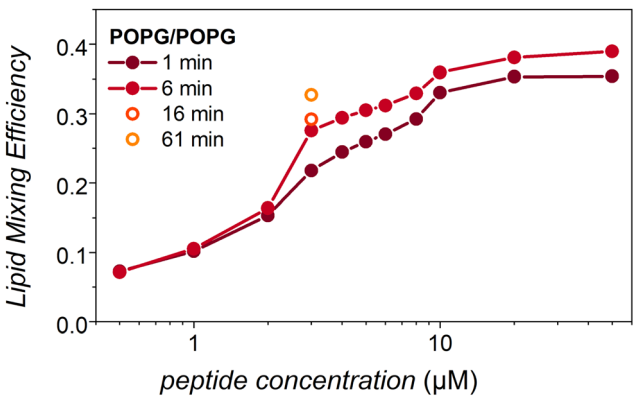

Fig. 4 Lipid mixing in POPE/POPG (50 : 50) vesicles induced by cR_3W_3 and measured after increasing incubation times as indicated. The experiments were performed in standard TRIS buffer at 25 °C. The depicted data is a typical example of three experiments conducted at slightly varying conditions (see Fig. S4, ESI†).

When vesicles contain 4% PEG-lipids, the particle size and size distribution do not change upon addition of peptide up to high concentrations (Fig. 3C). Vesicle aggregation and fusion are effectively prevented, although peptide binding does not appear to be affected (Fig. 6 in the ITC results below).

In POPG/POPE/DSPE-PEG_{2000} vesicles, the peptide induces a maximal total leakage of approximately 20% even after long incubation times and at high peptide concentration (Fig. 2D). This is significantly less than observed in POPG/POPE vesicles (Fig. 2A). Similar reduction in leakage when vesicles are decorated with PEG-chains was observed for melittin.[51] As in POPG/POPE vesicles without PEG-lipids, most leakage occurred within the first 10 minutes and there was only a small increase over time. A plateau in L_{total} is reached at peptide concentrations above 30 μM and an all-or-none leakage behavior is indicated by the lifetime of entrapped calcein τ_E (Fig. 2E). The τ_E values obtained below 0.4 ns might indicate that the vesicles are subjected to osmostic mismatch, resulting in water efflux and apparent increase in entrapped calcein concentration (*i.e.* decrease in τ_E) in the intact vesicles. Note also particularly large error bars in this part of the reciprocal plot.

Slow leakage in POPG/POPC vesicles

To examine the role of PE-lipids in binary model membranes, we used the less fusogenic but also zwitterionic lipid POPC in the vesicles instead of POPE and characterized the leakage induced by the peptide.

Fig. 2G–I show the total leakage induced by cR_3W_3 in POPG/POPC liposomes. Leakage increases, both, with increasing peptide concentration and over time. Another similarity between the leakage behavior of POPG/POPE and POPG/POPC vesicles is the all-or-none behavior (Fig. 2H). Compared to POPG/POPE, leakage occurs slower in POPG/POPC vesicles, *e.g.* less than 20% after 10 minutes incubation. Also, the total leakage at a given incubation time is lower. For instance, after the incubation of 30 μM peptide for 2 hours only 40% total vesicle leakage was measured. Taking into account only the reliable data, the leakage induced in POPG/POPC vesicles might require a higher peptide concentration than the leakage in POPG/POPE (Fig. 2G). The slow leakage depicted in Fig. 2I might indicate a slow (re-)occurrence of leakage events, not agreeing with what is expected for leaky fusion or leakage upon release of asymmetric-packing stress.[4]

As described for POPG/POPE vesicles, large and polydisperse particles also occurred in POPG/POPC vesicles after peptide addition (Fig. 3B). Therefore, we have incorporated 4% DSPE-PEG_{2000} into the vesicle membrane. Fig. 3D shows the constant particle size of POPG/POPC/DSPE-PEG_{2000} vesicles after peptide addition. Interestingly, this inhibition of aggregation and potential fusion did not reduce the vesicle leakage (Fig. 2J) compared to POPG/POPC without PEG-lipids. This is in contrast to the leakage behaviour observed in POPG/POPE and POPG/POPE/DSPE-PEG_{2000} vesicles. The difference in τ_E (Fig. 2H and K) is most likely attributable to slight osmotic mismatch of inside and outside buffer and the large error bars in this part of the graph.

It should be noted that POPG/POPC/DSPE-PEG_{2000} (50 : 50 : 4) vesicles are generally less stable than POPG/POPE/DSPE-PEG_{2000} (50 : 50 : 4) vesicles. In some preparations, the vesicles become leaky without addition of peptides.

PE also enhances leakage in CL containing vesicles

In order to assess the role of PG-lipids in model membranes, we exchanged two POPG by one TOCL lipid in the examined vesicles. These TOCL/POPE (1 : 2) membranes are expected to have the same charge density as a POPG/POPE (1 : 1) membrane.

After the addition of cR_3W_3 to TOCL/POPE vesicles, a similar increase in particle size and polydispersity was observed as for POPG/POPE vesicles (Fig. S6, ESI†). Therefore, the leakage behaviour can only be compared within short incubation times.

The substitution of PG by cardiolipin resulted in similar trends regarding the influence of the zwitterionic lipid on the

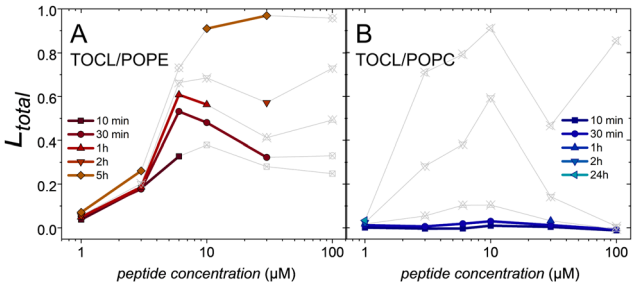

Fig. 5 Total leakage of (A) TOCL/POPE (1 : 2) and (B) TOCL/POPC (1 : 2) induced by cR_3W_3 as a function of peptide concentration at various incubation times. Data with a decrease in sum of B of more than 20% is omitted or depicted in grey. The experiments were performed in standard TRIS buffer at 25 °C.

leakage behavior. For TOCL/POPE vesicles, leakage occurred at a peptide concentration of 3 μM and reached a plateau between 6 and 10 μM (Fig. 5A). As in POPG/POPC, for TOCL/POPC, there is much less leakage after short incubation times (Fig. 5B).

Preparation of CL-containing vesicles containing 4% DSPE-PEG did not result in reliably stable vesicles.

cR_3W_3 binds to negatively charged model membranes

Isothermal titration calorimetry (ITC) experiments determine the heat response to the interaction between the antimicrobial peptide and model membranes. For this, the peptide was titrated into various liposome suspensions. All recorded heat responses were exothermic. Their integration resulted in sigmoidal curves, shown in Fig. 6.

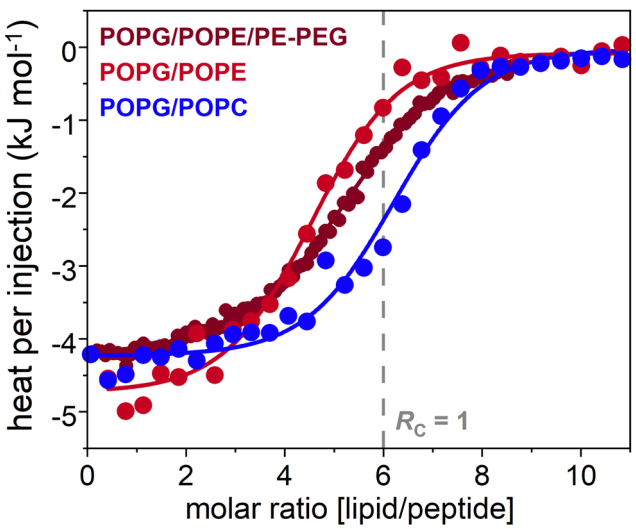

Fig. 6 Interaction of cR_3W_3 with model membranes analysed by isothermal titration calorimetry. 0.1 mM cR_3W_3 were injected into 5 mM POPG/POPC (50 : 50) (blue), 5 mM POPG/POPE (50 : 50) (red), and 4 mM POPG/POPE/DSPE-PEG_{2000} (50 : 50 : 4) (dark red) liposomes suspension, respectively. Dots represent the integrated heat per injection. Lines are guides for the eye. The charge neutralisation conditions are marked as R_c = 1. The experiments were performed in standard TRIS buffer at 25 °C. The depicted data is a typical example of three experiments conducted at similar conditions.

Here, we consider apparent binding affinity K (slope), stoichiometry n *i.e.* lipid : peptide ratio (midpoint), and enthalpy ΔH (amplitude) without dissecting the electrostatic and hydrophobic contributions to binding. A one-set-of-sites model was fitted to the isotherms (Table S1, ESI†). This probably oversimplified model yields acceptable fits but the absolute values should be considered with care.

cR_3W_3 binds to model membranes containing negatively charged PG-lipids with slightly exothermic reaction enthalpies between −4 and −5 kJ mol^{-1}, in agreement with Finger *et al.*[36] The difference between POPG/POPE, POPG/POPC, and POPG/POPE/DSPE-PEG_{2000} are marginal. Besides, the peptide binds to POPG/POPE membranes with an apparently higher stoichiometry (4.5 lipids per peptide) than to POPG/POPC membranes (6.1 lipids per peptide).

Considering mixed POPG/POPE membranes with 4 mol% PEG-lipids, there are only small differences in the binding properties compared to POPG/POPE membranes. This finding agrees with other reports.[5,33,52]

Discussion

Membrane permeabilization is commonly investigated as a potential mechanism by which antimicrobials harm microbes. So far, there have been no mechanistic model studies of potential membrane leakage caused by the cyclic hexapeptide used here. However, cR_3W_3 and related peptides have already been shown to induce electrostatic lipid clustering in mixed model membranes detectable by differential scanning calorimetry.[36] For these and other antimicrobials, this ability correlates with their antimicrobial activity.[10,36] Generally, it is difficult to judge the relevance of a given behavior such as clustering or leakage observed in model studies for the activity *in vivo*. Here, we challenge the role of the membrane model for the relevance of observed leakage for antimicrobial activity.

Given the molecular properties of the peptide, both, electrostatic interactions and some insertion of the peptide into the hydrophobic membrane core are expected. NMR analysis of a similar peptide suggests that the side chains point outwards with the backbone forming a rectangle, with two β-turns and the possibility of intramolecular hydrogen-bonds between residues apposing on the long sides. The aromatic side chains are found to point to the same direction, forming a hydrophobic region.[53] The peptide probably resides at the interface between the hydrophilic head groups and the hydrophobic membrane core, because of its small size and the tryptophan content, as well as the preference of the arginine side-chains to interact with phosphate groups. This is in agreement with increased surface pressures in lipid monolayers (Fig. S7, ESI†).

As described above, cR_3W_3 can induce substantial leakage in POPG/POPE vesicles and it is tempting to attribute the antimicrobial activity of the peptide to this membrane-related effect. As discussed below, we doubt a direct relevance of leaky fusion for antimicrobial activity. A minimal inhibitory concentration (MIC) for *E. coli* of 11 μM was reported.[7]

This concentration matches the active concentration determined by us. We consider this a coincidence. The peptide concentration in leakage experiments and the MIC should only be compared directly if the fraction of bound peptide is negligible ($c_{lipid} \cdot K \ll 1$), which is not the case here ($30\ \mu M \times 10^5\ M^{-1} \approx 3$, see Table S1, ESI†).[54,55] We will discuss more aspects of the leakage mechanism that will help to judge the relevance of the mechanistic model studies for processes, such as antimicrobial therapy or drug delivery.

In vesicles composed of the common bacterial lipids PG and PE, the leakage behavior induced by cR_3W_3 agrees with transient leakage that has been attributed to either asymmetric-packing stress or leakage upon fusion.[4] As will be discussed below, many indications point to leakage upon fusion as also observed for an antimicrobial polymer and in other cases.[5,30–32]

For more information on the leakage mechanism and the role of PE-lipids in model vesicles, three aspects will be discussed: (1) the role of aggregation and fusion for the observed leakage, (2) the role of the lipid composition for the leakage mechanism and membrane fusion. (3) We noticed severe problems with some of the fluorescence experiments and will discuss the success of various countermeasures.

(1) Most leakage in PG/PE is caused by leaky fusion

Indeed, there are several indications that the observed leakage is crucially influenced by aggregation and fusion, particularly leaky fusion induced by cR_3W_3 in POPG/POPE membranes.

To separate leakage from aggregation or leaky fusion, leakage is studied while aggregation, fusion, and similar effects are inhibited. This is done by preventing membrane–membrane contacts by sterical shielding of the vesicles with PEG-chains. No influence of PEG-lipids on the binding of the peptide to the lipid bilayer was observed in ITC (Fig. 6) and monolayer experiments (Fig. S7, ESI†). Regarding leakage, the presence of PEG-lipids is expected to result in either no changes, if the leakage mechanisms is independent of apparent fusion,[33] or a complete prevention of leakage if leakage only occurs *via* leaky fusion.[5] Different from these two reported cases, leakage induced by the cyclic peptide in POPG/POPE/DSPE-PEG_{2000} vesicles is significantly reduced compared to POPG/POPE vesicles, but not entirely abolished (Fig. 2A and D). Hence, the most plausible explanation is that the proportion of leakage that is prevented in the presence of PEG-lipids had been caused by leaky fusion. Indeed, computational simulations have yielded explanations for a high propensity of fusing membranes to develop defects close to the site of the fusion stalk.[56–58]

Leakage activity coincides with neutralization of the negative charges of the lipids by the positive charges of the peptides. At approximately 5 μM, the colloidal vesicles are not stabilized by charge repulsion any longer and aggregation is particularly favourable.[14–17] We assume that this pronounced aggregation promotes fusion and leaky fusion of the vesicles.

A complementary test for this hypothesis would be to enhance fusion of POPG/POPE vesicles at elevated vesicle density.[5] However, in the present case, these data are strongly influenced by changes in fluorescence intensity and difficult to evaluate reliably (details in the last paragraph of the ESI†).

Lipid mixing is observed, but can be quantified for short incubation times only (Fig. 4 and Fig. S5, ESI†). All our results indicate that most of the leakage observed in PG/PE vesicles is caused by leaky fusion.

Let us have yet another look at the leakage behavior in POPG/POPE vesicles. Interestingly, in the present case, some limited leakage is still observed when fusion is prevented in POPG/POPE/DSPE-PEG_{2000} vesicles. This suggests that two causes for leakage can superimpose: leaky fusion and another, independent mechanism. Supporting this interpretation, also the leakage observed in POPG/POPC membranes (Fig. 2G) suggests that cR_3W_3 can induce leakage by other mechanisms than leaky fusion. Nevertheless, there is a small chance that cR_3W_3 is a very strong fusogen and still induces limited fusion (and leaky fusion) in vesicles shielded with PEG-chains.

It is unusual that leakage is not exceeding 20%. Allende *et al.* attribute a similar reduction in leakage by PEG-chains to the formation of toroidal pores.[51]

The data in the second column in Fig. 2(B, E, H and K) indicate an all-or-none behavior, *i.e.* only a small part of the vesicles, or microbes, would be affected. How this translates to a potential microbial killing efficiency is difficult to assess.

(2) The role of lipid composition for the predominant leakage mechanism

For more insight to the role of the lipids in model membranes, we examined PG/PC instead of PG/PE mixtures. Vesicles composed of POPG/POPC (1 : 1) provide the same charge density as POPG/POPE (1 : 1), but are less fusogenic.[18] Apart from the slightly higher peptide concentration required, leakage in POPG/POPC seems similar to leakage in POPG/POPE at first sight. There is significant leakage, an increase in leakage over time, all-or-none behavior (Fig. 2A, B, G and H), and increased particle sizes (Fig. 3A and B) and changes in fluorescence intensity (Fig. S1, ESI†), indicating aggregation and potentially fusion. Because vesicles aggregation overcomes one of the barriers to vesicle fusion, it is possible that cR_3W_3 also induces fusion in POPG/POPC membranes even though PG/PC is much less prone to form stalk structures than PG/PE.

In fact, preventing aggregation or fusion in PG/PC vesicles by PEG-chains does not result in significant changes in leakage, when considering only the sound data (Fig. 2G and J). This comparison also exemplifies the potential overestimation of leakage because of aggregation, especially close to neutralization at approximately 5 μM peptide.

In more detail, in POPG/POPC, leakage is slower in the beginning of incubation compared to POPG/POPE. In POPG/POPC, significant leakage only starts after 30 minutes of incubation. This behavior is not in agreement with the time-scale of fusion or leakage by asymmetric-packing stress, which should evolve very quickly and stop within 1 hour of incubation.[4] Judged by the long leakage kinetics (Fig. 2I), leakage events occur and re-occur stochastically over a long period of time.[49] The leakage events might require a nucleation

step, oligomerization, a conformational change in the peptide, certain geometric arrangements *etc.* The small cyclic peptide does not have many possibilities for a conformational change, but an opening of intramolecular H-bonds that are indicated for a closely related peptide.[53]

Interestingly, the leakage mechanism seems more efficient in POPG/POPC or POPG/POPC/DSPE-PEG_{2000} than in POPG/POPE/DSPE-PEG_{2000}, even though binding of the peptide is very similar (Fig. 2D, G and 6). This observation agrees with our conclusion of different leakage mechanisms in PG/PE and PG/PC. Taken together, our data suggest that POPG/POPC is affected by a different leakage mechanism than leaky fusion, the main cause of leakage in POPG/POPE. More details of these leakage events can only be speculated: localized pores might be more probable than uniformly distributed, small defects. The latter would rather lead to homogeneous leakage in the entire vesicle population, *i.e.* gradual leakage.

Furthermore, we considered the role of the negatively charged lipid by exchanging PG for CL. The leakage data that can be considered safely supports the findings made with PG-containing membranes: leakage is fast in TOCL/POPE-mixtures and slow in TOCL/POPC-mixtures.

(3) Judging and improving the reliability and relevance of model studies

Limited relevance of the leaky fusion mechanism *in vivo*. Judging the relevance of leakage in model membranes for the activity in microbes, leaky fusion has to be regarded a special case among the many different leakage mechanisms, even though the cytoplasmic membrane is usually considered the target of membrane permeabilization. In fact, for closely related peptides, the cytoplasmic membrane of *B. subtilis* has been substantiated as target, but not for permeabilization.[38,42] In microbes, the outer layers, peptidoglycan or outer membranes of bacteria and microbial fungi probably prevent fusion of the cytoplasmic membranes. We think that leaky fusion itself is not the cause of the peptides antimicrobial activity. However, the disturbance of the membrane that proceeds to leaky fusion in model vesicles strongly suggests that there are significant membrane perturbations also in biological membranes, such as local membrane deformation that facilitates stalk structures. These might have implications for the integrity of microbial membranes,[59,60] so that leaky fusion in model vesicles may still be an indication of activity in microbes. Besides leakage, local alterations of membrane properties may affect the correct location and function of membrane proteins, as suggested before for a closely related peptide.[42] For judging or selecting membrane-active antimicrobials, we need to be aware that leaky fusion in model vesicles does not translate directly to leakage in microbes.

Different lipid composition in model membranes. We examined a POPG/POPC mixture as a less fusogenic variant of partially negatively charged model vesicles. These experiments indicate that cR_3W_3 can induce membrane permeabilization by another mechanism than leaky fusion and most probably not by asymmetric-packing stress. However, we need to keep in mind that replacing PE by PC might not only suppress fusion, but PC is also unable to engage in H-bonds, unlike PE acting as hydrogen donor or acceptor (NH_3^+, PO_2^-) and PG, CL acting as acceptors (PO_2^-) (Fig. 1).[61] Thus, it has been speculated that the pore-opening energy is lower in PC than in PE.[62]

Another lipid abundant in membranes of bacteria such as *S. aureus* is cardiolipin.[10] CL-containing vesicles filled with calcein were difficult to prepare, purify and use for leakage experiments. Because of the high preference of TOCL for negative spontaneous curvature, LUVs prepared of TOCL/POPE seem to be prone to premature leakage even below the transition temperature.[63] Nevertheless, model vesicles containing cardiolipin may be more stable with more complex lipid mixtures and useful to investigate the individual role of cardiolipin and the zwitterionic lipid component.

We consider it worthwhile to discuss problems that we encountered in the different fluorescence assays or those caused by the specific lipid and peptide components of our study.

Increased particle sizes caused by aggregation. The vesicles used here are stabilized as colloids by their charges. Their neutralization by the added peptides results in severe aggregation and in some cases also in fusion.[14–17,21]

Aggregation of charged vesicles suggests that also bacteria would be agglutinated – not mediated by their cytoplasmic membranes, but by negatively charged components on the outermost layers of their envelops. It has been suggested before, that bacterial agglutination contributes to antimicrobial activity.[64–66]

Increased particle sizes have important technical implications. When vesicles aggregate or even floculate (Fig. S2, ESI†), several effects can lead to decreases in fluorescent counts or fluorescence intensity. The aggregates could sediment or float out of the beam, turbidity and light scattering can influence fluorescence intensity in unpredictable ways. This is especially problematic when the changes in absolute fluorescence intensity are the actual read-out. This can be the case, for example, in FRET or quenching-based assays, such as the intensity-based leakage assay. This leakage assay examines increased fluorescence intensity upon dilution of self-quenching dyes and normalizes all data to solubilized vesicles assumed to denote the end-point. It is difficult to judge whether the fluorescence intensity is compromised by aggregates that might affect each data point differently. In addition to expectable problems with fluorescence intensity, we observed here that also lifetime-based fluorescence measurements can be severely affected. Nevertheless, lifetime-based fluorescence measurements have advantages. For example, an unexpected decrease in fluorescent counts because of aggregation can easily be monitored *via* the pre-exponential factors of the fit to the decay (sum of B, eqn (3) and Fig. S1, ESI†). Additionally, all-or-none or graded leakage behavior and longer incubation times can be examined without the need for more samples, which is more convenient than in steady-state experiments.

Aggregation is a very unpredictable effect with particle sizes varying widely between individual preparations. Light scattering is therefore not reproducible and difficult to correct

for. In less severe cases, the reliability of the fluorescence intensity can be improved using relative intensities. This can lead to a successful quantification of lipid mixing efficiency, for example.[5,46]

We explored several countermeasures to aggregation and fusion, such as steric shielding by PEG-lipids, using a less fusogenic lipid composition, using intensity ratios, and assessing data reliability using the sum of B as measure for the effective calcein concentration. None of them is perfect.

PEG-lipids are not always a straightforward strategy against vesicle aggregation. PEG-ylated vesicles are widely used in pharmaceutical approaches and have been proposed to prevent unwanted vesicle aggregation and fusion.[17,50,51] We have experienced here that DSPE-PEG_{2000} cannot be added to all lipid compositions without additional effects or even problems. In particular, mixtures of POPG/POPC seemed vulnerable to premature leakage if 4 mol% DSPE-PEG_{2000} were present. This is underlined by monolayer experiments, where discrepancies in the minimal area per lipid after compression indicates loss of material into the subphase (Fig. S8, ESI†). Problems with extrusion, foaming and premature leakage of vesicles composed of TOCL/POPE/DSPE-PEG_{2000} or TOCL/POPC/DSPE-PEG_{2000} indicate that these lipid mixtures do not support stable LUVs.

FRET and tryptophan side chains. Not only the behavior of the lipid vesicles can affect fluorescent studies. In the FRET-based lipid mixing assay that we intended to use to quantify membrane fusion, we encountered cross talk between the tryptophan side chains in cR_3W_3 and the FRET pair (Fig. S5, ESI†). These effects cannot be easily corrected for.

Conclusions

The example peptide presented here induced leakage in model membranes of various compositions including PG/PE and PG/PC membranes. It is, thus, easy to suspect a role of membrane permeabilization in the antimicrobial activity of cR_3W_3. Detailed analysis reveals different leakage mechanisms, such as leaky fusion in POPG/POPE vesicles and leakage independent of fusion in vesicles with a different lipid composition. While leakage independent of fusion probably contributes to antimicrobial activity in microbes, leaky fusion might not even occur in microbes, and thus might be irrelevant for the application in antimicrobial therapy.

We suspect, that leakage in PG/PE model membranes does not explain the main cause of antimicrobial activity of cR_3W_3. Furthermore, we would like to advocate the detailed characterization of leakage behaviour beyond the active concentration range and extent.

Especially, we would like to draw attention to a potential bias of model vesicles to leaky fusion, because membrane fusion and the related leakage cannot occur in microbes and might only contribute indirectly to antimicrobial activity. The effect of leaky fusion might therefore harmonize earlier work on a closely related cyclic peptide reporting leakage in model membranes but not in bacteria.[2,7,42] Moreover, leaky fusion might occur in more cases beyond the specific compounds investigated here or reported earlier.[5,30–32]

There are several options to preclude or test for leaky fusion as we have shown: prevention or enhancement of vesicle aggregation, changing for a lipid composition that is less prone to fusion (*i.e.* involving PC-lipids instead of PE-lipids), or experimental setups that prevent vesicle–vesicle contacts, such as free standing membranes, isolated giant vesicles, *etc.*

As discussed in detail above, it is worthwhile to consider varying the lipid composition for mechanistic model studies. Matching the exact composition of the microbial cytoplasmic membrane might not be the ideal option. Especially PG/PE mixtures without outer cell wall components or peptidoglycan layers are prone to fusion, an effect that is less relevant in microbes. Other lipids, such as cardiolipins, abundant in *S. aureus*, or the use of PEG-lipids might cause additional problems such as unstable vesicles.

Having in mind the diverse experimental problems we encountered, it seems indispensable to monitor data quality by a parameter such as the sum of pre-exponential factors, or to check for unexpected changes in fluorescence intensity otherwise. First indications of fusion can be obtained by light scattering, cryo-transmission electron microscopy, or fluorescence-based fusion assays. When antimicrobial activity is to be understood, being aware of leaky fusion is important.

Experiments with PG/PE and PG/PC vesicles yielded very valuable information about the ability of cR_3W_3 to induce different types of leakage behaviour.

With this mechanistic knowledge, it is easier to judge the relevance of leakage behavior in model membranes for *in vivo* situations and to avoid misleading conclusions in antimicrobial efficacy and mechanism of action studies. Furthermore, certain leakage behavior can be avoided or modified purposefully. For instance, leakage can be enhanced or reduced by modulating the fusion propensity of the lipid membrane or the membrane-active compound.

Author contributions

KB and JN performed experiments and data analyses. MH acquired funding, supervised data analysis, and lead writing and editing of the manuscript. All authors contributed to the manuscript.

Conflicts of interest

There are no conflicts to declare.

Acknowledgements

We gratefully acknowledge access to instrumentation by the Heerklotz lab. This work was funded by the German Research Foundation (DFG 415894560).

References

1 Y. Shai, *Pept. Sci.*, 2002, **66**, 236–248.
2 K. Scheinpflug, O. Krylova, H. Nikolenko, C. Thurm and M. Dathe, *PLoS One*, 2015, **10**, e0125056.
3 S. Guha, J. Ghimire, E. Wu and W. C. Wimley, *Chem. Rev.*, 2019, **119**, 6040–6085.
4 W. C. Wimley and K. Hristova, *Aust. J. Chem.*, 2020, **73**, 96–103.
5 S. Shi, H. Fan and M. Hoernke, *Nanoscale Adv.*, 2022, **4**, 5109–5122.
6 A. Stulz, A. Vogt, J. S. Saar, L. Akil, K. Lienkamp and M. Hoernke, *Langmuir*, 2019, **35**, 16366–16376.
7 C. Junkes, R. D. Harvey, K. D. Bruce, R. Dölling, M. Bagheri and M. Dathe, *Eur. Biophys. J.*, 2011, **40**, 515–528.
8 H. Choi, N. Rangarajan and J. C. Weisshaar, *Trends Microbiol.*, 2016, **24**, 111–122.
9 C. Ratledge and S. G. Wilkinson, *Microbial lipids*, Academic press, 1988, vol. 2.
10 R. M. Epand and R. F. Epand, *J. Pept. Sci.*, 2011, **17**, 298–305.
11 F. Savini, S. Bobone, D. Roversi, M. L. Mangoni and L. Stella, *Pept. Sci.*, 2018, **110**, e24041.
12 S. L. Leikin, M. M. Kozlov, L. V. Chernomordik, V. S. Markin and Y. A. Chizmadzhev, *J. Theor. Biol.*, 1987, **129**, 411–425.
13 A. Witkowska, L. P. Heinz, H. Grubmüller and R. Jahn, *Nat. Commun.*, 2021, **12**, 3606.
14 J. E. Cummings and T. K. Vanderlick, *Biochim. Biophys. Acta, Biomembr.*, 2007, **1768**, 1796–1804.
15 D. Volodkin, V. Ball, P. Schaaf, J.-C. Voegel and H. Mohwald, *Biochim. Biophys. Acta, Biomembr.*, 2007, **1768**, 280–290.
16 F. Quemeneur, M. Rinaudo, G. Maret and B. Pépin-Donat, *Soft Matter*, 2010, **6**, 4471–4481.
17 T. M. Domingues, B. Mattei, J. Seelig, K. R. Perez, A. Miranda and K. A. Riske, *Langmuir*, 2013, **29**, 8609–8618.
18 C. S. Poojari, K. C. Scherer and J. S. Hub, *Nat. Commun.*, 2021, **12**, 1–10.
19 B. P. Navas, K. Lohner, G. Deutsch, E. Sevcsik, K. Riske, R. Dimova, P. Garidel and G. Pabst, *Biochim. Biophys. Acta, Biomembr.*, 2005, **1716**, 40–48.
20 Y. G. Smirnova, H. J. Risselada and M. Müller, *Proc. Natl. Acad. Sci. U. S. A.*, 2019, **116**, 2571–2576.
21 T. M. Domingues, K. R. Perez and K. A. Riske, *Langmuir*, 2020, **36**, 5145–5155.
22 L. Marx, E. F. Semeraro, J. Mandl, J. Kremser, M. P. Frewein, N. Malanovic, K. Lohner and G. Pabst, *Front. Med. Technol.*, 2021, **3**, 2.
23 L. Sun, K. Hristova and W. C. Wimley, *Nanoscale*, 2021, **13**, 12185–12197.
24 S. L. Hanna, J. L. Huang, A. J. Swinton, G. A. Caputo and T. D. Vaden, *Biophys. Chem.*, 2017, **227**, 1–7.
25 Y. Cajal, O. G. Berg and M. K. Jain, *Biochem. Biophys. Res. Commun.*, 1995, **210**, 746–752.
26 G. D. Eytan, R. Broza and Y. Shalitin, *Biochim. Biophys. Acta, Biomembr.*, 1988, **937**, 387–397.
27 G. Fujii, D. Eisenberg and M. E. Selsted, *Protein Sci.*, 1993, **2**, 1301–1312.
28 X.-F. Xia, F. Zhang, P.-C. Shaw and S.-F. Sui, *IUBMB Life*, 2003, **55**, 681–687.
29 I. Kabelka, M. Pachler, S. Prévost, I. Letofsky-Papst, K. Lohner, G. Pabst and R. Vácha, *Biophys. J.*, 2020, **118**, 612–623.
30 A.-V. Villar, A. Alonso and F. M. Goñi, *Biochemistry*, 2000, **39**, 14012–14018.
31 S.-T. Yang, E. Zaitseva, L. V. Chernomordik and K. Melikov, *Biophys. J.*, 2010, **99**, 2525–2533.
32 D. J. Brock, H. Kondow-McConaghy, J. Allen, Z. Brkljača, L. Kustigian, M. Jiang, J. Zhang, H. Rye, M. Vazdar and J.-P. Pellois, *Cell Chem. Biol.*, 2020, **27**, 1296–1307.
33 S. Shi, A. M. Markl, Z. Lu, R. Liu and M. Hoernke, *Langmuir*, 2022, **38**, 2379–2391.
34 A. Bortolotti, C. Troiano, S. Bobone, M. M. Konai, C. Ghosh, G. Bocchinfuso, Y. Acharya, V. Santucci, S. Bonacorsi, C. Di Stefano, J. Haldar and L. Stella, *Biochim. Biophys. Acta, Biomembr.*, 2023, **1865**, 184079.
35 M. Dathe, H. Nikolenko, J. Klose and M. Bienert, *Biochemistry*, 2004, **43**, 9140–9150.
36 S. Finger, A. Kerth, M. Dathe and A. Blume, *Biochim. Biophys. Acta, Biomembr.*, 2015, **1848**, 2998–3006.
37 S. Finger, A. M. Kerth, M. Dathe and A. Blume, *Biochim. Biophys. Acta, Biomembr.*, 2020, **1862**, 183248.
38 M. Wenzel, A. I. Chiriac, A. Otto, D. Zweytick, C. May, C. Schumacher, R. Gust, H. B. Albada, M. Penkova and U. Krämer, *et al.*, *Proc. Natl. Acad. Sci. U. S. A.*, 2014, **111**, E1409–E1418.
39 B. Claro, E. González-Freire, M. Calvelo, L. J. Bessa, E. Goormaghtigh, M. Amorn, J. R. Granja, R. Garcia-Fandiño and M. Bastos, *Colloids Surf., B*, 2020, **196**, 111349.
40 N. Schmidt, A. Mishra, G. H. Lai and G. C. Wong, *FEBS Lett.*, 2010, **584**, 1806–1813.
41 S. Futaki and I. Nakase, *Acc. Chem. Res.*, 2017, **50**, 2449–2456.
42 K. Scheinpflug, M. Wenzel, O. Krylova, J. E. Bandow, M. Dathe and H. Strahl, *Sci. Rep.*, 2017, **7**, 44332.
43 G. R. Bartlett, *J. Biol. Chem.*, 1959, **234**, 466–468.
44 H. Patel, C. Tscheka and H. Heerklotz, *Soft Matter*, 2009, **5**, 2849–2851.
45 D. K. Struck, D. Hoekstra and R. E. Pagano, *Biochemistry*, 1981, **20**, 4093–4099.
46 N. Düzgünes, T. M. Allen, J. Fedor and D. Papahadjopoulos, *Biochemistry*, 1987, **26**, 8435–8442.
47 A. S. Ladokhin, W. C. Wimley and S. H. White, *Biophys. J.*, 1995, **69**, 1964–1971.
48 W. C. Wimley, M. E. Selsted and S. H. White, *Protein Sci.*, 1994, **3**, 1362–1373.
49 C. Mazzuca, B. Orioni, M. Coletta, F. Formaggio, C. Toniolo, G. Maulucci, M. D. Spirito, B. Pispisa, M. Venanzi and L. Stella, *Biophys. J.*, 2010, **99**, 1791–1800.
50 A. K. Kenworthy, K. Hristova, D. Needham and T. J. McIntosh, *Biophys. J.*, 1995, **68**, 1921–1936.
51 D. Allende, S. A. Simon and T. J. McIntosh, *Biophys. J.*, 2005, **88**, 1828–1837.
52 S. Rex, J. Bian, J. R. Silvius and M. Lafleur, *Biochim. Biophys. Acta, Biomembr.*, 2002, **1558**, 211–221.

53 C. Appelt, A. Wessolowski, M. Dathe and P. Schmieder, *J. Pept. Sci.*, 2008, **14**, 524–527.
54 H. Heerklotz and S. Keller, *Biophys. J.*, 2013, **105**, 2607–2610.
55 F. Savini, V. Luca, A. Bocedi, R. Massoud, Y. Park, M. L. Mangoni and L. Stella, *ACS Chem. Biol.*, 2017, **12**, 52–56.
56 K. Katsov, M. Müller and M. Schick, *Biophys. J.*, 2006, **90**, 915–926.
57 H. J. Risselada, G. Bubnis and H. Grubmüller, *Proc. Natl. Acad. Sci. U. S. A.*, 2014, **111**, 11043–11048.
58 B. Bu, M. Crowe, J. Diao, B. Ji and D. Li, *Soft Matter*, 2018, **14**, 5277–5282.
59 A. Hickel, S. Danner-Pongratz, H. Amenitsch, G. Degovics, M. Rappolt, K. Lohner and G. Pabst, *Biochim. Biophys. Acta, Biomembr.*, 2008, **1778**, 2325–2333.
60 D. Zweytick, S. Tumer, S. E. Blondelle and K. Lohner, *Biochem. Biophys. Res. Commun.*, 2008, **369**, 395–400.
61 P. Garidel and A. Blume, *Eur. Biophys. J.*, 2000, **28**, 629–638.
62 S. Bobone, D. Roversi, L. Giordano, M. De Zotti, F. Formaggio, C. Toniolo, Y. Park and L. Stella, *Biochemistry*, 2012, **51**, 10124–10126.
63 D. P. Siegel, *Biophys. J.*, 1999, **76**, 291–313.
64 A. Marquette, B. Lorber and B. Bechinger, *Biophys. J.*, 2010, **98**, 2544–2553.
65 E. Robert, T. Lefevre, M. Fillion, B. Martial, J. Dionne and M. Auger, *Biochemistry*, 2015, **54**, 3932–3941.
66 C. Muñoz-Camargo, V. S. Montoya, L. A. Barrero-Guevara, H. Groot and E. Boix, 2018 IX International Seminar of Biomedical Engineering (SIB), 2018, pp. 1–5.